

Anisotropic light emissions in luminescent solar concentrators— isotropic systems

Paul P. C. Verbunt,¹ Carlos Sánchez-Somolinos,² Dirk J. Broer,¹ and Michael G. Debije^{1,*}

¹Functional Materials & Devices, Chemical Engineering & Chemistry, Eindhoven University of Technology, 5600 MB Eindhoven, The Netherlands

²Instituto de Ciencia de Materiales de Aragón, Universidad de Zaragoza-CSIC, Departamento de Física de la Materia Condensada C./Pedro Cerbuna 12, 50009-Zaragoza, Spain

*m.g.debije@tue.nl

Abstract: In this paper we develop a model to describe the emission profile from randomly oriented dichroic dye molecules in a luminescent solar concentrator (LSC) waveguide as a function of incoming light direction. The resulting emission is non-isotropic, in contradiction to what is used in almost all previous simulations on the performance of LSCs, and helps explain the large surface losses measured in these devices. To achieve more precise LSC performance simulations we suggest that the dichroic nature of the dyes must be included in the future modeling efforts.

©2013 Optical Society of America

OCIS codes: (350.6050) Solar energy; (160.2540) Fluorescent and luminescent materials.

References and links

1. W. H. Weber and J. Lambe, "Luminescent greenhouse collector for solar radiation," *Appl. Opt.* **15**(10), 2299–2300 (1976).
2. A. Goetzberger, "Fluorescent solar energy collectors operating conditions with diffuse light," *Appl. Phys. (Berl.)* **16**(4), 399–404 (1978).
3. M. G. Debije and P. P. C. Verbunt, "Thirty years of luminescent solar concentrator research: solar energy for the built environment," *Adv. En. Mater.* **2**(1), 12–35 (2012).
4. See www.bouwiqonline.nl, BouwiQ 2012/2 (accessed March 2013), for example.
5. L. H. Slooff, E. E. Bende, A. R. Burgers, T. Budel, M. Pravettoni, R. P. Kenny, E. D. Dunlop, and A. Büchtemann, "A luminescent solar concentrator with 7.1% power conversion efficiency," *Phys. Status Solidi* **2**(6), 257–259 (2008).
6. J. C. Goldschmidt, M. Peters, A. Bösch, H. Helmers, F. Dimroth, S. W. Glunz, and G. P. Willeke, "Increasing the efficiency of fluorescent concentrator systems," *Sol. Energy Mater. Sol. Cells* **93**(2), 176–182 (2009).
7. L. Desmet, A. J. M. Ras, D. K. G. de Boer, and M. G. Debije, "Monocrystalline silicon photovoltaic luminescent solar concentrator with 4.2% power conversion efficiency," *Opt. Lett.* **37**(15), 3087–3089 (2012).
8. N. Yamada, L. N. Anh, and T. Kambayashi, "Escaping losses of diffuse light emitted by luminescent dyes doped in micro/nanostructured solar cell systems," *Sol. Energy Mater. Sol. Cells* **94**(3), 413–419 (2010).
9. J. C. Goldschmidt, M. Peters, L. Prönneke, L. Steidl, R. Zentel, B. Bläsi, A. Gombert, S. W. Glunz, G. P. Willeke, and U. Rau, "Theoretical and experimental analysis of photonic structures for fluorescent concentrators with increased efficiencies," *Phys. Status Solidi* **205**(12), 2811–2821 (2008) (a).
10. M. Carrascosa, S. Unamuno, and F. Agullo-Lopez, "Monte Carlo simulation of the performance of PMMA luminescent solar collectors," *Appl. Opt.* **22**(20), 3236–3241 (1983).
11. M. van Gorp and Y. K. Levine, "Determination of transition moment directions in molecules of low symmetry using polarized fluorescence. I. Theory," *J. Chem. Phys.* **90**(8), 4095–4102 (1989).
12. M. van Gorp, T. van Heijnsbergen, G. van Ginkel, and Y. K. Levine, "Determination of transition moment directions in molecules of low symmetry using polarized fluorescence. II. Applications to pyranine, perylene, and DPH," *J. Chem. Phys.* **90**(8), 4103–4111 (1989).
13. C. Sánchez, B. Villacampa, R. Cases, R. Alcalá, C. Martínez, L. Oriol, and M. Piñol, "Polarized photoluminescence and order parameters of 'in situ' photopolymerized liquid crystal films," *J. Appl. Phys.* **87**(1), 274–279 (2000).
14. A. M. Hermann, "Luminescent solar concentrators - a review," *Sol. Energy* **29**(4), 323–329 (1982).
15. M. G. Debije, P. P. C. Verbunt, B. C. Rowan, B. S. Richards, and T. L. Hoeks, "Measured surface loss from luminescent solar concentrator waveguides," *Appl. Opt.* **47**(36), 6763–6768 (2008).
16. L. R. Wilson, B. C. Rowan, N. Robertson, O. Moudam, A. C. Jones, and B. S. Richards, "Characterization and reduction of reabsorption losses in luminescent solar concentrators," *Appl. Opt.* **49**(9), 1651–1661 (2010).

17. B. S. Richards and K. R. McIntosh, "Overcoming the poor short wavelength spectral response of CdS/CdTe photovoltaic modules via luminescence down-shifting: ray-tracing simulations," *Prog. Photovolt. Res. Appl.* **15**(1), 27–34 (2007).
 18. A. A. Earp, G. B. Smith, P. D. Swift, and J. Franklin, "Maximising the light output of a luminescent solar concentrator," *Sol. Energy* **76**(6), 655–667 (2004).
 19. P. P. C. Verbunt, A. Kaiser, K. Hermans, C. W. M. Bastiaansen, D. J. Broer, and M. G. Debije, "Controlling light emission in luminescent solar concentrators through use of dye molecules planarly aligned by liquid crystals," *Adv. Funct. Mater.* **19**(17), 2714–2719 (2009).
 20. C. L. Mulder, P. D. Reusswig, A. P. Beyler, H. Kim, C. Rotschild, and M. A. Baldo, "Dye alignment in luminescent solar concentrators: II. Horizontal alignment for energy harvesting in linear polarizers," *Opt. Express* **18**(S1), A91–A99 (2010).
 21. R. W. MacQueen, Y. Y. Cheng, R. G. C. R. Clady, and T. W. Schmidt, "Towards an aligned luminophore solar concentrator," *Opt. Express* **18**(S2 Suppl 2), A161–A166 (2010).
 22. S. McDowall, B. L. Johnson, and D. L. Patrick, "Simulations of luminescent solar concentrators: Effects of polarization and fluorophore alignment," *J. Appl. Phys.* **108**(5), 053508 (2010).
-

1. Introduction

The luminescent solar concentrator (LSC), first described in the late 1970's [1,2], has been gaining renewed interest as a potential source of electricity generation from sunlight for use in the built environment, an area which has very difficult operating conditions and aesthetic demands not easily met by traditional photovoltaic (PV) panels [3]. In principle, the LSC is simple: it consists of a plastic or glass plate acting as a waveguide. The waveguide is either filled with luminescent materials, or topped by a thin layer containing the luminophores. The luminophores absorb incident sunlight, and re-emit the light at a longer wavelength. A fraction of the emitted light is trapped in the waveguide by total internal reflection. Some of the emission light reaches the edge(s) of the waveguide, where small PV cells are attached to convert the light into electrical current. The LSC performs similarly under both cloudy and sunny conditions, and can be colored and produced in a variety of shapes and sizes, making integration into the urban setting much easier, as it allows the designer more opportunities to exercise their artistic vision [4].

Widespread adoption of the device has not yet occurred for one primary reason: the electrical generation efficiency has only been modest [5–7]. Photons emitted by luminophore molecules inside the LSC waveguides will only be totally internally reflected if they encounter the waveguide-air interface at angles larger than the critical angle. The photons with smaller angles with respect to the normal of the waveguide surfaces will be lost through the top and/or bottom. The trapping efficiency of emitted photons depends not only on the material of the waveguide but also on the angular distribution of the emitted photons. This distribution is assumed to be spherical in most previous literature [8–10]. In this work, a model is presented that calculates the angular distribution of photons emitted by dye molecules isotropically distributed in a host material (dye ensemble), and the importance of this distribution is discussed.

2. Calculation of angular distribution of emitted photons from isotropically distributed dichroic dye molecules

Organic dyes are π -conjugated molecules. The molecular cores are mostly planar with the transition dipole moments for absorption and emission usually contained in the conjugation plane. This leads to anisotropic molecular absorption and therefore linear absorption dichroism in ordered samples. Similarly, the angular distribution of emitted photons from one molecule or an ensemble of oriented molecules is not isotropic. The absorption probability of incoming light depends on the angle of the transition dipole for absorption (μ) with respect to the polarization of the incoming light (\vec{e}_i). The probability for emission depends on the transition dipole for emission (ν) and the polarization of the emitted light (\vec{e}_f). The angular

distribution of the intensity ($I(\alpha, \beta)$) of the emitted light from an ensemble of dye molecules (Ω) can be defined as

$$I(\alpha, \beta) \propto \left\langle \left(\vec{e}_i \cdot \vec{\mu} \right)^2 \left(\vec{e}_f \cdot \vec{\nu} \right)^2 \right\rangle_{\Omega} \quad (1)$$

where α and β denote the polar and azimuthal angle of the emitted light and the brackets represent the average over all positions of the dye molecules [11–13]. It is assumed that the direction of the transition dipoles for absorption and emission are the same, and that the dye molecules are static during the lifetime of the excited state (that is, the emission is faster than the molecular motions). Using these assumptions, the angular distribution of the emitted photons will be [11]

$$I(\alpha, \beta) \propto \left\langle \left(\vec{e}_i \cdot \vec{\mu} \right)^2 \left(\vec{e}_f \cdot \vec{\mu} \right)^2 \right\rangle_{\Omega}. \quad (2)$$

When there are aggregates of dye molecules formed or re-absorption and sequential re-emission events occur, this assumption is no longer valid. In Fig. 1(a) a schematic definition is given for the transition dipole for absorption of a dye molecule when illuminated from the top by collimated sunlight.

Sunlight may be treated as unpolarized. Dye molecules that lack a chiral center have no intrinsic preference for the handedness of circular polarized light, making it possible to mimic unpolarized light with circular polarized light. The transition dipole and the polarization of the incoming light are defined as:

$$\vec{\mu} = \begin{pmatrix} \sin \theta \cos \varphi \\ \sin \theta \sin \varphi \\ \cos \theta \end{pmatrix}, \quad \vec{e}_i = \frac{1}{\sqrt{2}} \begin{pmatrix} 1 \\ i \\ 0 \end{pmatrix} \quad (3)$$

The propagation direction of light emitted by a dye molecule (\vec{k} , Eq. (4)) depends on

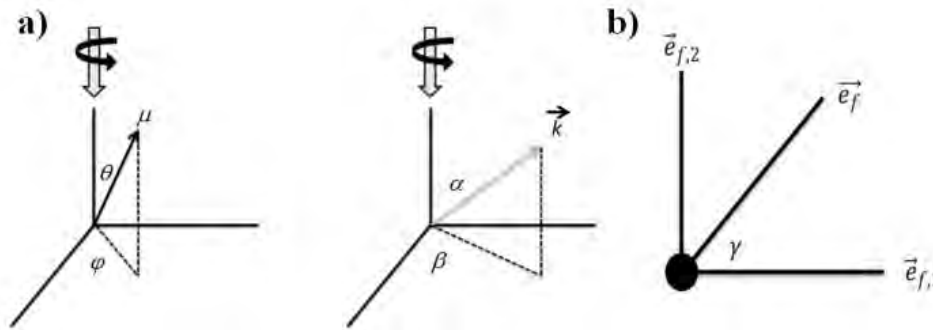


Fig. 1. a) Schematic definition of the dipole, the incoming light and the emitted light for both the absorption (left) event and the emission (right) event. In the left Fig. the black arrow represents the dipole moment for absorption defined by a zenith (θ) and an azimuthal (φ) angle with respect to the axis system. In the right image the emitted photon (\vec{k}) is also defined by a zenith (α) and an azimuthal (β) angle with respect to the axis system. The large grey arrow in both pictures represents the direction of the incoming light which is circularly polarized (curved black arrow). b) polarization of the emitted light as function of two linear polarizations orthogonal to \vec{k} .

the polarization of this light (\vec{e}_f). This polarization of the emitted light can be described in a dielectric media by a linear combination of two linear polarizations ($\vec{e}_{f,1}$ and $\vec{e}_{f,2}$) orthogonal to \vec{k} (see Fig. 1(b), where \vec{k} is perpendicular to the plane).

$$\vec{k} = \begin{pmatrix} \sin \alpha \cos \beta \\ \sin \alpha \sin \beta \\ \cos \alpha \end{pmatrix} \quad (4)$$

The two linear polarizations orthogonal to \vec{k} are defined as

$$\vec{e}_{f,1} = \begin{pmatrix} -\cos \alpha \cos \beta \\ -\cos \alpha \sin \beta \\ \sin \alpha \end{pmatrix} \quad (5)$$

$$\vec{e}_{f,2} = \begin{pmatrix} -\sin \beta \\ -\cos \beta \\ 0 \end{pmatrix}$$

so the polarization of the emitted light is

$$\vec{e}_f = \begin{pmatrix} -\cos \gamma \cos \alpha \cos \beta - \sin \gamma \sin \beta \\ -\cos \gamma \cos \alpha \sin \beta + \sin \gamma \cos \beta \\ \cos \gamma \sin \alpha \end{pmatrix} \quad (6)$$

The definitions of γ , $\vec{e}_{f,1}$ and $\vec{e}_{f,2}$ are depicted in Fig. 1(b).

The emitted light will have all polarizations so the calculation of the intensity of this emitted light becomes

$$I(\alpha, \beta) \propto \int_0^{2\pi} \left\langle \left(\vec{e}_i \cdot \vec{\mu} \right)^2 \left(\vec{e}_f \cdot \vec{\mu} \right)^2 \right\rangle_{\Omega} d\gamma \quad (7)$$

The average over the ensemble of dye molecules can then be described by

$$I(\alpha, \beta) = \int_0^{2\pi} d\gamma \int_0^{2\pi} d\varphi \int_0^{\pi} d\theta \sin \theta f(\Omega) \left(\left(\vec{e}_i \cdot \vec{\mu} \right)^2 \left(\vec{e}_f \cdot \vec{\mu} \right)^2 \right) \quad (8)$$

where $f(\Omega)$ is the distribution function of the transition dipoles within the ensemble. Random distributions of dichroic dye molecules have isotropically distributed transition dipoles. The distribution function can be described as $f(\Omega) = p$, where p is a constant. Combining this with Eq. (3), (6), and (8), and calculating all integrals leads to the angular distribution of the emitted photons

$$I(\alpha, \beta) \propto (3 + \cos^2 \alpha) \quad (9)$$

This angular distribution of emitted photons from an isotropic dichroic dye system illuminated by collimated light from directly overhead is depicted in Fig. 2.

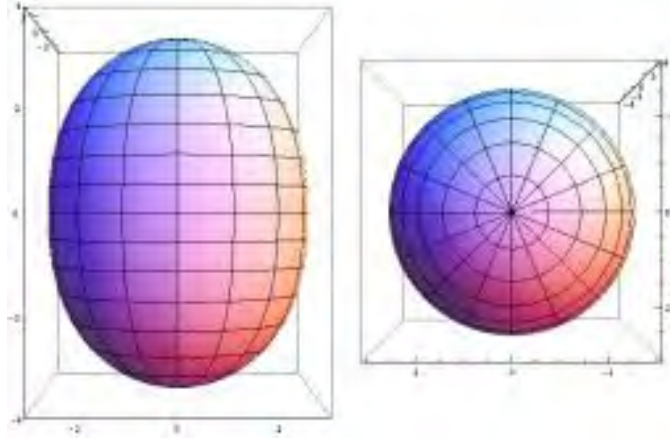


Fig. 2. Emission profile from isotropic dye ensembles illuminated from the top, both the side view (left) and the top view (right). The axis of these emission profile have arbitrary units. The units are the same on both axes and the emission originates from the center of the profile.

The distribution will change its orientation when the direction of incoming light is varied. For example, the calculated emission from a dye ensemble illuminated by direct light incident from an angle of 50 degrees to the normal is depicted in Fig. 3 below.

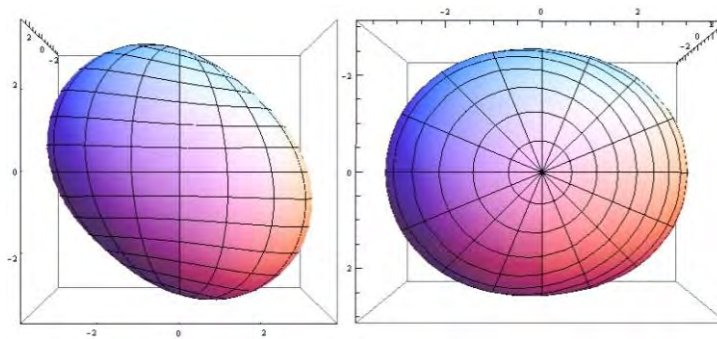


Fig. 3. Emission profile from isotropic dye ensembles illuminated at a 50 degree angle to the surface normal, both the side view (left) and the top view (right). The axis of these emission profile have arbitrary units. The units are the same on both axes and the emission originates from the center of the profile.

3. Discussion

The emission profiles depicted in Figs. 2 and 3 may be significant for determining the ultimate potential performance of the LSC device. As mentioned in the Introduction above, it has been generally assumed isotropic emissions from dye ensembles so that about 25% of emitted photons will escape from the surface of an LSC. This assumption is correct if applied to an isotropic emitter such as a phosphor, or to a dichroic dye-containing system illuminated equally from all directions. However, for the normal configuration of an LSC device, this is not a correct assumption. Most LSCs described in the literature make use of dichroic dyes, and almost all are exposed to the sun which is incident from one side, and generally from a single direction. In this latter situation, dye molecules lying with their absorption dipole oriented parallel to the normal of the waveguide will absorb almost no light, meaning there will be less light directed into the plane of the waveguide. Molecules with dipole axes perpendicular to the waveguide normal will absorb a lot of light, but a significant fraction of the emission will be directed so as to escape the top and bottom surfaces.

After the initial absorption/emission event, the description of a real system gets much more difficult, as reabsorption, caused by the limited Stokes shift (separation between the absorption and emission wavelengths of the dye materials), starts to play its rôle. The emission light encountering dye molecules within the waveguide that may be reabsorbed will approach these dyes with a limited angular distribution, favoring a particular range of orientations. This will again result in non-uniform emission distributions.

In an LSC only those emitted photons reaching the waveguide-air interface with angles larger than the critical angle will be total internally reflected, while photons with a smaller angle with respect to the normal of the interface are lost through the surface. Since the LSC is normally positioned in air the critical angle (α_c) is dependent on the refractive index of the waveguide (n), and can be approximated by

$$\alpha_c = \sin^{-1}\left(\frac{1}{n}\right) \quad (10)$$

In the literature the emission of the dye molecules has often been assumed to be isotropic, and the fraction of emitted light trapped in the waveguide (η_{trap}) is described as [14]

$$\eta_{trap} = \cos(\alpha_c) = \left(1 - \frac{1}{n^2}\right)^{1/2} \quad (11)$$

Standard polymer waveguide materials used in LSCs are PMMA and PC, which have refractive indices of approximately 1.49 and 1.58, respectively, leading to trapping efficiencies of 74.1% and 77.4%.

The amount of photons lost through the surface of an LSC depends on this trapping fraction. Every (re-)absorption and subsequent emission event, a part of the emitted photons is lost through the surface equal to $1 - \eta_{trap}$. When one assumes the fraction of photons transported through the host material of the LSC and the fraction of waveguided photons reflected at the waveguide surfaces (dictated by the smoothness of the surface) are unity, the total fraction of the number of absorbed photons that is lost through the surfaces of an LSC with an isotropic emitter can be calculated by:

$$\eta_{sl} = \sum_{i=0}^{\bar{x}} \eta_{PL}^{i+1} \left(\eta_{trap}^i (1 - \eta_{trap}) \right) \quad (12)$$

where \bar{x} is the average number of photon reabsorption/reemission events and η_{PL} represents the probability an absorbed photon be re-emitted by the fluorescent dye molecule. In Table 1 the surface loss of an LSC with an isotropic emitter with an η_{PL} of 1.0 is shown as a function of \bar{x} .

Results from the model presented in Section 3 above showed the emission from LSCs with dichroic dyes in an isotropic host illuminated with collimated light normal to the plane of the LSC is not isotropic. Using this non-isotropic emission profile, the fraction of emitted light trapped in the waveguide can be calculated using

$$\eta_{trap,0} = \frac{\int_0^{2\pi} d\beta \int_{\alpha_c}^{\pi-\alpha_c} d\alpha I(\alpha, \beta) \sin \alpha}{\int_0^{2\pi} d\beta \int_0^{\pi} d\alpha I(\alpha, \beta) \sin \alpha} \quad (13)$$

where, $I(\alpha, \beta)$ is the emission profile. The 0 in the index of the trapping fraction denotes that this is the trapping fraction of the light emitted after the initial absorption and emission event, so only emission is taken into account after absorption of the incident sunlight and no photon

reabsorption is considered. The initial trapped fraction for a dichroic dye in an isotropic host is 0.743 in PC and 0.708 in PMMA.

As shown in Section 2, the emission profile of an isotropic dye ensemble will change as the angle of incidence is varied. The change in emission profile will result in a change in initial trapped fraction of emitted photons in a waveguide. The initial trapped fraction of emitted photons as function of the angle of the incident light is depicted in Fig. 4, demonstrating increased trapping with increasing angle of incidence. At these larger incidence angles, the probability of sunlight absorption by the dye molecules in the LSC also increases due to a longer pathlength of the incident photons through the dye containing waveguide or layer, suggesting indirect illumination of the LSC could have a positive impact on trapping probability.

Since the emission profile is dependent on the distribution of the light absorbed, the profile will change every time a photon is reabsorbed and re-emitted, leading to an increase in trapped fraction each subsequent event. The fractional surface loss for a dichroic dye may be described by:

$$\eta_{sl} = \eta_{PL} (1 - \eta_{trap,0}) + \eta_{PL}^2 (\eta_{trap,0} (1 - \eta_{trap,1})) + \eta_{PL}^3 (\eta_{trap,0} \eta_{trap,1} (1 - \eta_{trap,2})) + \dots \quad (14)$$

where the index of the trapping efficiency denotes the number of the photon reabsorption/re-emission events which redistribute the photons (0 denotes the initial absorption and

Table 1. Theoretical fractional surface loss from LSCs with an isotropic emitter as a function of number of reabsorption/re-emission events.

x	Surface loss	
	PC	PMMA
0	0.226	0.259
1	0.398	0.451
2	0.534	0.593
3	0.638	0.699

emission of incident sunlight). The incident light is considered to be collimated in one single direction, but the emitted light that will be re-absorbed will have a very different distribution increasingly isotropic as shown in Fig. 2. For isotropic incident light, the emission from isotropically distributed dichroic dyes will be isotropic as well. This means that with each photon recycling event the trapping fraction will become closer to the trapping fraction of an isotropic emitter.

In Fig. 5 the surface loss for dichroic dyes and isotropic emitters is plotted as function of the number of photon reabsorption/re-emission events using Eq. (12), where the trapped fraction is kept constant at 0.743 and 0.708 for the dichroic dye in PC and PMMA respectively. The calculated surface loss from the LSC with the dichroic dyes is an estimate: our formulation is not easily able to accurately model re-absorption events past the first due to the complications of expressing the light distributions and dichroic dye alignment vectors in a

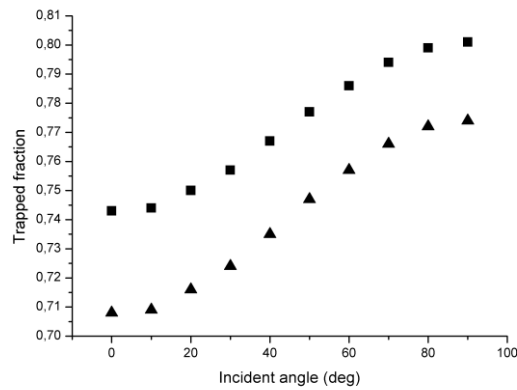


Fig. 4. The initial fraction of photons emitted by isotropic dichroic dye ensembles trapped in a polycarbonate (squares) or a PMMA (triangles) waveguide when illuminated with sunlight at different incident angles with respect to the waveguide normal.

workable set of equations. However, these results are consistent with the losses described in our earlier work [15].

Our model predicted the fraction of absorbed photons trapped in the waveguide is 0.743, so 25.7% is emitted in surface loss mode if only the initial absorption of sunlight is taken into account (no reabsorption). Earlier work on waveguides filled with or topped by the dye Lumogen Red 305, a standard dye commonly used for LSC work [3], demonstrated surface losses of 40% of the absorbed energy, which translated to more than 50% of the absorbed photons. From these earlier measurements, we estimate the number of photon reabsorption/re-emission events for filled PC waveguides should be around 1.4-1.6 (2.4-2.6 total dye interactions for each photon) for the dichroic dye model and approximately 2 (3 total dye interactions for each photon) for the isotropic emitter model for the experimental data to match the models.

The number of photon recycling events is determined by the concentration of dye molecules in the waveguide, limited by the degree of overlap in absorption and emission band. Each photon recycling event results in the photon losing energy. After a number of re-

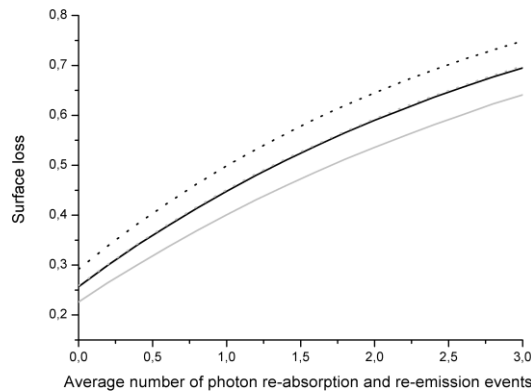


Fig. 5. Calculated surface loss from LSCs as function of the average number of photon reabsorption/re-emission events for PC (grey) and PMMA (black) waveguides containing isotropic emitters (solid lines) or dichroic dyes (dotted lines). The lines of isotropic emitters in PMMA (solid black) and dichroic emitters in PC (dotted grey) are almost coincident.

absorptions the emitted photon will not have sufficient energy to re-excite another dye molecule and cannot be reabsorbed any more. Simulations performed at the Herriot-Watt University using software based on Monte Carlo simulations have shown that the number of dye interactions of each photon is at most 1.8 [16,17]. These simulations were performed without considering the extended absorption tail of the dye molecules for low energy photons [16,18], thus the number of re-absorptions are probably slightly higher than the 1.8 predicted, although the impact for the size of the samples studied ($5 \times 5 \text{ cm}^2$) will likely be small. However, for large samples the influence of this tail will be greater [18].

Including the dichroic nature of these organic dyes is important if one is to make accurate predictions of the behavior of LSC systems. That dye alignment has an impact on the emission of a LSC waveguide system has been verified in experiments employing liquid crystals as the aligning medium [19–21] and is also supported by Monte-Carlo simulations [22]. Planar alignment, for example, resulted in emission light exiting primarily two waveguide edges. Models and simulations that assume isotropic dye emission will not be able to reproduce such results. With this in mind, we will adapt our simulation to be able to calculate the effects of arbitrary dye alignments on the distribution of emitted light, and will present this in a future publication.

4. Conclusions

The emission profile for randomly oriented dichroic dye molecules in an isotropic host illuminated with collimated light is not isotropic, although it has been treated as isotropic in simulations designed to estimate LSC performance. When one assumed the absorption and emission transition moments are coincident in the active dichroic dye molecule, and assuming no rotational diffusion during the fluorescence lifetime, emission of photons is predicted to lead to additional surface losses from the LSCs, supporting earlier experimental findings. Changing the direction of the incoming sunlight influences the emission profile of the isotropically oriented dichroic dyes, which will also impact the waveguiding of these emissions, and the subsequent degree of reabsorption. Future simulations of LSCs should include the dichroic nature of the luminophores in absorption and emission for accurate calculations for both direct and indirect sun lighting conditions.

Acknowledgments

M.D. would like to acknowledge the support of STW Vidi grant 7940 and C.S.S. thanks the Spanish MINECO project MAT2011-27978-C02-02, CSIC project i-LINK0394, Gobierno de Aragón, and FEDER (EU). The authors would like to thank Dick de Boer of Philips Research for his advice on the simulations and Ties de Jong of the Eindhoven University of Technology and Paul Urbach of the Delft University of Technology for their helpful insights and comments.